Acta Geotechnica (2017) 12:225–230
DOI 10.1007/s11440-016-0439-7

SHORT COMMUNICATION

A monotonic bounding surface critical state model for clays

Jinbo Chen[1,2,3]

Received: 23 March 2015 / Accepted: 20 January 2016 / Published online: 16 February 2016

Abstract This study investigates a simple constitutive model based on the critical state framework and bounding surface (*BS*) plasticity that is suitable for reconstituted clays over a wide range of overconsolidation ratios under monotonic loading. For heavily overconsolidated (*OC*) clays, rather than using the conventional Hvorslev line, an empirical surface is introduced into the model formulation based on two image points on the *BS*. The peak strength and the dilatancy of heavily *OC* clays can thus be predicted satisfactorily. Comparisons with triaxial test data show that the model well captures the peak strength and the dilatancy of heavily *OC* clays under monotonic loading.

Keywords Clay · Constitutive model · Critical state · Overconsolidated · Peak strength

1 Introduction

Realistic models of the mechanical behavior of soils with reasonable material inputs are essential in the application of numerical methods for solving geotechnical problems. Most of the existing constitutive models for clays are based on the critical state framework [1]. Although the modified Cam clay (*MCC*) model [2] performs satisfactorily for normally consolidated (*NC*) and lightly overconsolidated (*OC*) clays [3, 4], it suffers from a major limitation in that the strength is largely overestimated on the dry side.

Significant research efforts have been made to improve the accuracy of the *MCC* model on the dry side. On the one hand, comprehensive models with rigorous mathematical derivations consistent with the plasticity theory are available in the literature for analyzing the behavior of heavily *OC* clays and soils under cyclic loading, e.g., the kinematic hardening models with two or more surfaces [5, 6], the bubble models with kinematic yield surfaces within the outer surface [7, 8], the shear sliding-compression double-yield-surface model [9], the bounding surface (*BS*)-based anisotropic hardening MIT-E3 model [10], the elegant thermomechanics-based model capable of constructing a family of models [11]. On the other hand, experiment-based empirical expressions for the peak strength of heavily *OC* are widely used. Hvorslev [12] found through experiments that a straight line satisfactorily approximated the peak strength for heavily *OC* soils, which was used by Atkinson and Bransby [13] in an elasto-plastic model and Yao et al. [14] in a subloading model on the dry side. However, a straight line such as the Hvorslev line to represent the peak strength of unbonded heavily *OC* clays is intrinsically unsafe at certain conditions [15]. Therefore, a revised parabolic Hvorslev curve was proposed by Yao et al. [16] for highly *OC* clays. A comprehensive evaluation of the performance of four common constitutive models for remolded clays was presented by Bryson and Salehian [17].

The objectives of this study are to derive an empirical experiment-based surface and to incorporate the derived surface into a simple monotonic constitutive model to capture the behavior of heavily *OC* clays. The peak strength-state parameter relation proposed by Atkinson

✉ Jinbo Chen
cvechenjinbo@gmail.com

1 Centre for Offshore Research & Engineering, National University of Singapore, Singapore, Singapore

2 Department of Civil and Environmental Engineering, National University of Singapore, 1 Engineering Drive 2, #08-23, Blk E1, 117576 Singapore, Singapore

3 Present Address: The University of Texas at Austin, Austin, TX, USA

[15] based on extensive experimental data is formulated in the effective stress space to give a reference surface governing the peak strength of heavily *OC* clays. Rather than using the straight Hvorslev line, this reference surface is incorporated into the model formulation. In this manner, the peak strength of heavily *OC* clays can be satisfactorily represented while the simplicity of the *MCC* model is retained.

2 Constitutive relation

2.1 The incremental theory of elasto-plasticity

The widely accepted incremental form of the stress–strain relation under monotonic loading following Potts and Zdravkovic [18] is

$$\{d\sigma'\} = \left\{ [D^e] - \frac{[D^e]\left\{\frac{\partial P}{\partial \sigma'}\right\}\left\{\frac{\partial F}{\partial \sigma'}\right\}^T [D^e]}{H + \left\{\frac{\partial F}{\partial \sigma'}\right\}^T [D^e]\left\{\frac{\partial P}{\partial \sigma'}\right\}} \right\}\{d\varepsilon\} \quad (1)$$

where $\{d\sigma'\}$ and $\{d\varepsilon\}$ are the effective stress increment vector and the total strain increment vector, respectively. The prime (′) denotes 'effective'. $[D^e]$ is the elastic stiffness matrix, $\{\partial F/\partial\sigma'\}$ and $\{\partial P/\partial\sigma'\}$ are, respectively, the outward directions of the yield surface (or the *BS* in the current study) F and the plastic potential P.

The model is formulated in the triaxial space (p', q, v), where p' and q are, respectively, the mean effective stress and the deviatoric stress. v is the specific volume. The conventional definitions of $\{p', q\}$ and the strains $\{\varepsilon_v, \varepsilon_q\}$ will be used [1], where ε_v and ε_q are the volumetric and deviatoric strains, respectively.

2.2 Bounding surface, flow rule and hardening rule

A generalized form of the yield surface in the *MCC* model is used to describe the *BS* in the model as show in Eq. (1) and Fig. 1.

$$\text{Wet side}: F = \frac{q^2}{M^2} + \frac{4}{R_w^2}\left(p' - \frac{2}{2+R_w}p'_c\right)^2 - \left(\frac{2}{2+R_w}p'_c\right)^2 = 0 \quad (2a)$$

$$\text{Dry side}: F = \frac{q^2}{M^2} + \left(p' - \frac{2}{2+R_w}p'_c\right)^2 - \left(\frac{2}{2+R_w}p'_c\right)^2 = 0 \quad (2b)$$

where M is the slope of the critical state line (*CSL*) in the $p' - q$ space, p'_c is the intercept of the *BS* with the p' axis, termed the pre-consolidated pressure. R_w is a material parameter for determining the mean effective stress at the critical state p'_{cr} such that $p'_{cr} = 2p'/(2 + R_w)$.

To maintain the simplicity of the proposed model, the associated flow rule is used. Hence $\{\partial F/\partial\sigma'\} = \{\partial P/\partial\sigma'\}$. $\{\partial F/\partial\sigma'\}$ is evaluated at the first image point $B_1(\bar{p}'_1, \bar{q}_1)$, which is the intersection of the *BS* with a straight line connecting the origin of the stress space O and the current stress point $A(p', q)$ as shown in Fig. 1. The overbar in $(\bar{p}'_1, \bar{q}_1)$ indicates that the coordinates lie on the *BS* as will be used throughout this paper. The volumetric hardening rule as the *MCC* model is adopted, i.e., $dp'_c/p'_c = v d\varepsilon_v^p/(\lambda - \kappa)$, where λ and κ are, respectively, the slopes of the isotropic normal compression line and the swelling line in the $v - \ln p'$ space, and ε_v^p is the plastic volumetric strain.

2.3 Peak strength of heavily *OC* clays

Generally, *NC* and lightly *OC* clays will compress or tend to compress under shearing. The peak stress will not occur before reaching the critical state under monotonic loading [1, 19]. Heavily *OC* clays, however, will dilate and soften during drained shearing. Thus, the strength will reach a peak before decreasing to the critical state. For unbonded soils, a curve is required to represent the peak strength from $p' = 0$ to the critical state in the $p' - q$ space [15]. Therefore, a reference surface, which is derived from the empirical criterion proposed by Atkinson [15] based on extensive experimental data, is incorporated in the current model to capture the peak strength of heavily *OC* clays under monotonic loading as shown in Eq. 3 (see 'Appendix' section)

$$\frac{q}{Mp'} = 1 + \beta \ln\left(\frac{p'_{cr}}{p'}\right) \quad (3)$$

where β is the peak strength parameter. If $\beta = 1$, Eq. (3) gives the dry-side yield surface of the original Cam clay model [1]. Thus, the reference surface is not a stationary

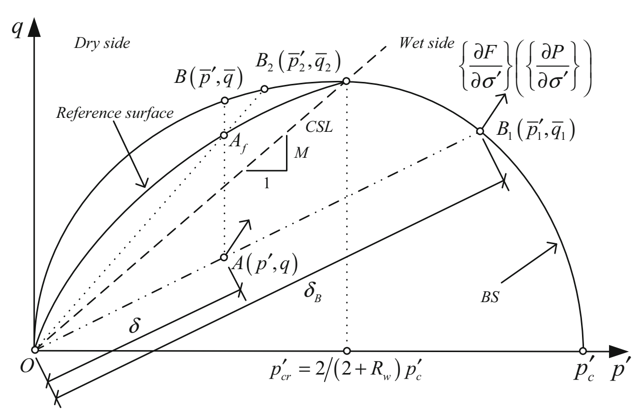

Fig. 1 *BS* and image points

surface in the stress space but will expand or contract with the *BS* according to the accumulated plastic strain.

2.4 Plastic modulus

The plastic modulus H used in the elasto-plastic stiffness matrix is defined as

$$H = (H_1 - \omega \xi H_2)\left(1 + \Omega \frac{\delta_B - \delta}{\delta_B}\right)^{\gamma} \quad (4)$$

where $H1$ and $H2$ are the plastic moduli, respectively, calculated following the conventional elasto-plasticity theory when $A(p', q)$ coincides with $B_1(\bar{p'}_1, \bar{q}_1)$ and $B_2(\bar{p'}_2, \bar{q}_2)$. $B_2(\bar{p'}_2, \bar{q}_2)$ is the second image point on the *BS* determined in a manner similar to that for $B_1(\bar{p'}_1, \bar{q}_1)$ with a line connecting O and A_f as shown in Fig. 1. A_f is the vertical projection of $A(p', q)$ on the reference surface. δ_B and δ are, respectively, the distances from O to $B_1(\bar{p'}_1, \bar{q}_1)$ and $A(p', q)$ as shown in Fig. 1. γ is a material parameter termed the plastic modulus parameter. ω, ξ and Ω are state variables, defined as $\omega = \left(M^2 + \bar{\eta}_2^2\right)/\left(M^2 + \bar{\eta}_1^2\right), \xi = [(\bar{\eta}_B - \bar{\eta}_1)/(\bar{\eta}_B - \bar{\eta}_2)]^{0.2}$ and $\Omega = \left(\zeta_1^2 + \zeta_2^2\right)^{-0.5}$. $\bar{\eta}_1, \bar{\eta}_2$ and $\bar{\eta}_B$ are the stress ratios (defined as the ratio of the deviatoric stress to the mean effective stress), respectively, at $B_1(\bar{p'}_1, \bar{q}_1), B_2(\bar{p'}_2, \bar{q}_2)$ and $B(\bar{p'}, \bar{q})$. $B(\bar{p'}, \bar{q})$ is the vertical projection of $A(p', q)$ on the *BS*. ζ_1 and ζ_2, respectively, represent the deviations of the mean effective stress and the deviatoric stress from the initial loading point, which are similar to those presented by Pestana and Whittle [20] as $\zeta_1 = \max\left[1 - p'_0/p', 1 - p'/p'_0\right]$ and $\zeta_2 = \left[3/2\left(\boldsymbol{s}/p' - \boldsymbol{s}_0/p'_0\right) : \left(\boldsymbol{s}/p' - \boldsymbol{s}_0/p'_0\right)\right]^{0.5}$. p_0' and $\boldsymbol{s}_0$ are the initial mean effective stress and the initial deviatoric stress tensor, respectively. $\boldsymbol{s}$ is the current deviatoric stress tensor. ':' is the tensor scalar product.

The basic philosophy of the proposed plastic modulus is to incorporate the reference surface to more accurately represent the peak strength of heavily *OC* clays. In the general case, before $A(p', q)$ reaches the reference surface, $H > 0$. Thus, the shear stress will increase during further shearing (softening can also occur when significant dilation and contraction of the reference surface occur in undrained shearing). If $A(p', q)$ lies on the reference surface (e.g., drained shearing), $H = 0$, and the peak stress state is reached. After reaching the peak stress state, because of the dilation on the dry side, the *BS* and the reference surface will contract during further loading, resulting in a negative value of the plastic modulus. Thus, the soil state enters the post-peak zone before reaching the critical state. ω ensures that the plastic modulus will be positive before the reference surface is reached. ξ ensures the consistency condition, i.e., when $A(p', q)$ approaches $B_1\left(\bar{p'_1}, \bar{q}_1\right)$, H degenerates to H_1. Ω is introduced so that H becomes load path dependent, and the soil behaves elastically immediately after initial loading beneath the *BS*. This behavior is consistent with the Masing effect, in which the elastic zone moves with the current stress [4].

3 Model evaluation

3.1 Model parameters determination

Generally, the proposed model has eight material parameters: N, λ, κ, M, μ', R_w, γ, β, where N is the intercept of the *CSL* with the v-axis in the $v - \ln p'$ space and μ' is the effective Poisson's ratio. The elastic bulk modulus of the model is evaluated the same as the *MCC* model. The first five parameters are the same as those in the *MCC* model. M is assumed to depend on the Lode's angle, although the transformed stress method is also proposed in the literature [21]. R_w is intended to give a general shape of the *BS*. The value can be determined from the triaxial, isotropic, consolidated undrained/drained (*CIU/CID*) tests on *NC* clays. γ governs the evolution of the plastic modulus and is similar to that presented by Zienkiewicz et al. [22]. Typical values of γ fall in the range of 2–8. β governs the nonlinearity of the evolution of the peak strength of heavily *OC* clays. It is preferable to determine β from drained shearing tests since heavily *OC* clays will exhibit a well-defined peak strength in drained shearing tests [19]. In *CID* tests or in triaxial, isotropic, consolidated constant p' (*CICP*) tests, β is determined as

$$\text{CID tests}: \beta = \frac{M_p - M}{M \ln\left[\frac{2\left(3 - M_p\right)}{3(2 + R_w)} \frac{p'_{cp}}{p'_0}\right]} \quad (5a)$$

$$\text{CICP tests}: \beta = \frac{M_p - M}{M \ln\left(\frac{2}{2 + R_w} \frac{p'_{cp}}{p'_0}\right)} \quad (5b)$$

where M_p is the measured peak stress ratio and p'_{cp} is the pre-consolidation pressure at the peak stress state. However, p'_{cp} depends on the plastic strain accumulated before the peak stress state is reached. A first estimate of $p_{\bar{c}p} = 0.9p'_{c0}$ (where p'_{c0} is the initial pre-consolidation pressure) could be used, and subsequent parametric studies would be necessary to refine the value.

3.2 Simulation of *CIU* tests

The *CIU* test on the heavily *OC* kaolin clay is simulated, and the comparisons with the test data presented by Banerjee and Stipho [23, 24] are made. The *CIU* compression (*CIUC*) test for *NC* clay was used to determine R_w. γ was

Table 1 Summary of model parameters used in proposed model

Clay type	N	v_0	λ	κ	M	μ'	R_w	γ	β
Kaolin clay [23, 24]	–	1.95	0.14	0.05	1.05-compression 0.85-extension	0.20	3.6	4	0.60
Fujinomori clay [25]	2.24	–	0.09	0.02	1.36-compression 1.0-extension	0.20	2.0	2	0.18

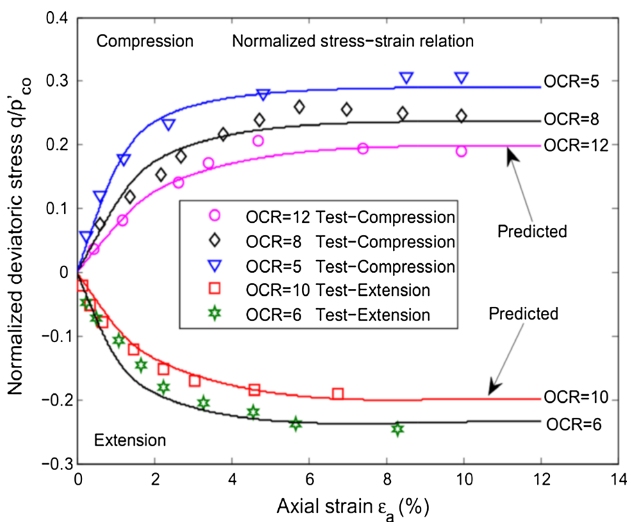

Fig. 2 Comparison of measured and predicted results for stress–strain relation in *CIU* test

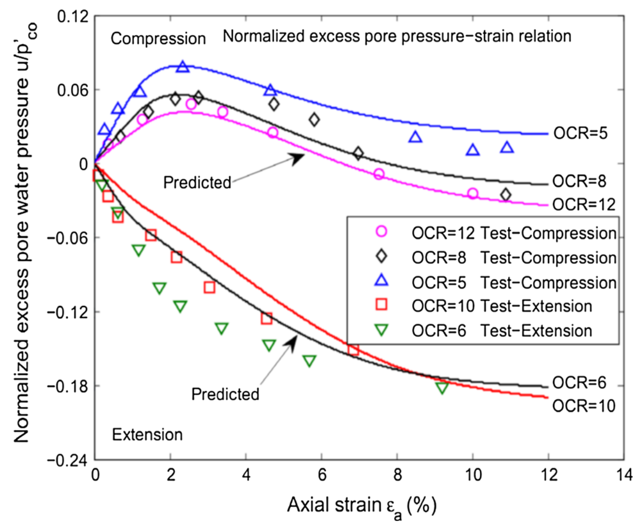

Fig. 3 Comparison of excess pore pressure in *CIU* test

evaluated by fitting the effective stress path for OCR = 1.2 [23]. β was determined by fitting the overall stress–strain data from the *CIUC* test for $OCR = 12$. The remaining parameters were obtained from the original study and are summarized in Table 1, where v_0 is the initial specific volume. As can be seen from Fig. 2, the predicted normalized stress–strain curves are consistent with the test data. In the *CIUC* tests, the model accurately predicts both the strength and the stiffness at all *OCRs*, although the slight softening exhibited at $OCR = 8$ and 12 is not predicted. In the *CIU* extension (*CIUE*) tests, the model predictions are generally consistent with the test results for both the stiffness and the strength.

Figure 3 shows a comparison of the predicted normalized excess pore water pressure with the test data. In the *CIUC* tests, the results are consistent. The excess pore water pressure decreased significantly at larger strains during tests because of the dilation. This behavior is accurately predicted by the proposed model. In the *CIUE* tests, the predicted dilatancy in the initial loading for both *OCRs* is less than that of the test results. At larger axial strains, the predicted dilatancy is reasonably consistent.

3.3 Simulation of *CICP* tests

The *CICP* test on the Fujinomori clay is simulated, and the comparisons with the test data published by Nakai and Hinokio [25] are made. R_w was determined from the test on *NC* clay. γ was determined by fitting the stress–strain data of the *CICP* compression test for $OCR = 2$, and β was evaluated from the *CICP* compression test data for $OCR = 8$ and Eq. (5). The remaining parameters were obtained from the original study and are summarized in Table 1. Figure 4 shows a comparison of the model predictions with the test data for the *CICP* compression test. Because the test results for $OCR = 8$ and 2 were used to calibrate the model, it is expected that the predicted stress–strain relations would be close. For the test with $OCR = 4$, the predicted values of the peak strength are slightly higher than the experimental values. For the test on *NC* clay, the model degenerates to the *MCC* model, and the results are consistent. For the volumetric behavior, the predictions for $OCR = 1$ and 2 are reasonably consistent with the test data. For the tests with $OCR = 4$ and 8, the predicted dilatancy at the early stage of loading is slightly lower than the actual results.

A comparison of the model predictions with the test data in the *CICP* extension test is shown in Fig. 5. For the stress–strain relations, the results are consistent for both the

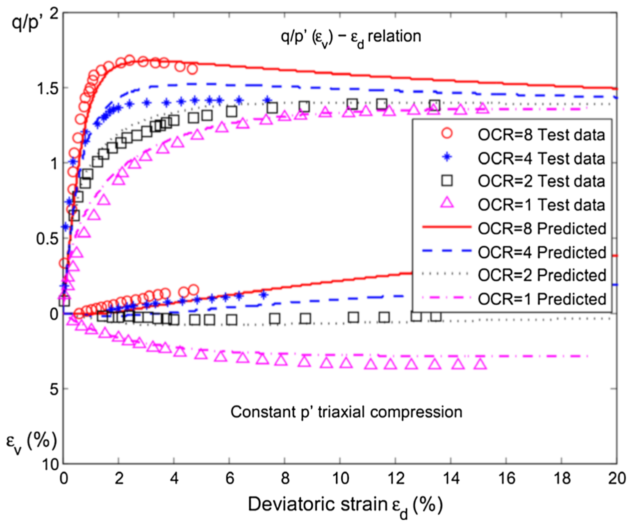

Fig. 4 Comparison of measured and predicted results for *CICP* compression test

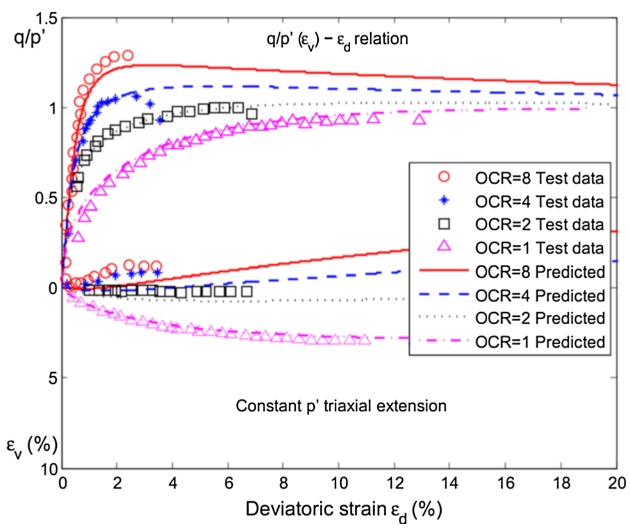

Fig. 5 Comparison of measured and predicted results for *CICP* extension test

stiffness and the peak strength, although the predicted values of the peak strength for $OCR = 8$ are slightly lower than the test values. Similar to the *CICP* compression test, the predicted results for the volumetric behavior for $OCR = 1$ and 2 are satisfactory, but the predicted dilatancy for $OCR = 4$ and 8 at the early stage of loading is lower.

4 Conclusion

The *MCC* model provides a rational framework for understanding the soil behavior. The proposed model improves the predictions on the dry side by employing a load path dependent plastic modulus and an empirically determined reference surface. Comparisons of model predictions with triaxial test data of different kinds of clays under undrained and drained conditions were made. The predicted results for the peak strength and the volumetric behavior of the clays over a wide range of *OCRs* under monotonic loading are consistent with the test data, which justify the proposed reference surface and the plastic modulus; however, the associated flow rule used by the current model neglects the impact of the soil density on the dilatancy of clays. Hence the model needs to be refined in order to improve the dilatancy prediction and to further consider cyclic loading.

Acknowledgments The author would like to thank Professor Chow Yean Khow, Professor Choo Yoo Sang and Dr. Goh Siang Huat of the National University of Singapore for many fruitful discussions on the model and the Lloyd's Register Foundation (LRF) for the support through the Centre for Offshore Research and Engineering at the National University of Singapore.

Appendix

Atkinson [15] proposed a criterion for the peak strength of heavily overconsolidated clays as follows:

$$\frac{q}{Mp'} = 1 + \frac{\beta}{\lambda - \kappa}\xi_d \tag{6}$$

where ξ_d is the state parameter measuring the vertical distance between the current stress point $A(v, p')$ and the *CSL* in the $v - \ln p'$ space. β is the peak strength parameter. From Fig. 6, the following equation holds:

$$\xi_d = \Gamma - v_\kappa = \lambda \ln\left(\frac{p'_{cr\_v}}{p'}\right) \tag{7}$$

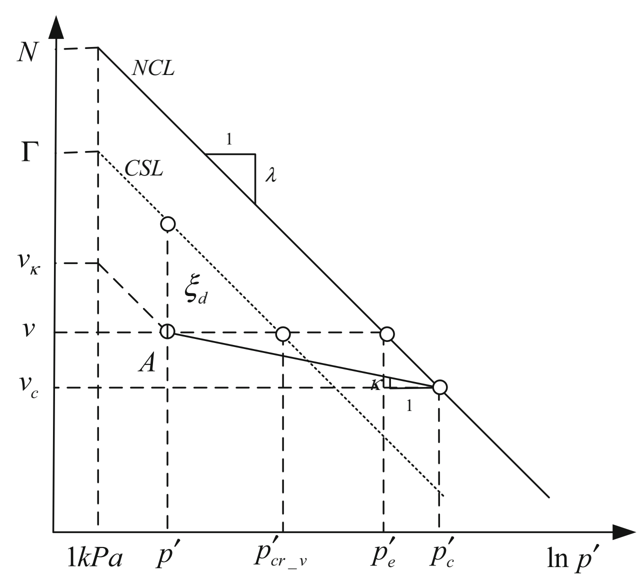

Fig. 6 Stress state in $v - \ln p'$ space

where Γ is the intercept of the CSL with the v-axis in the $v - \ln p'$ space. v_κ is the intercept of a line, which passes through $A(v, p')$ and parallels with the CSL, with the v-axis in the $v - \ln p'$ space. p'_{cr_v} is the mean effective stress on the CSL at the current specific volume v, and is determined through:

$$v = \Gamma - \lambda \ln p'_{cr\_v} \tag{8}$$

Substituting Eq. (7) into (6) yields

$$\frac{q}{Mp'} = 1 + \beta \frac{\lambda}{\lambda - \kappa} \ln\left(\frac{p'_{cr\_v}}{p'}\right) \tag{9}$$

v can also be specified through the isotropic normal compression line (NCL) as follows:

$$v = N - \lambda \ln p'_e \tag{10}$$

where N is the intercept of the CSL with the v-axis in the $v - \ln p'$ space. $p_e{}'$ is the equivalent pressure, the effective pressure on the NCL at v. Combining Eq. (8) with (10) gives

$$\ln p'_{cr\_v} = \frac{\Gamma - N}{\lambda} + \ln p'_e \tag{11}$$

From Fig. 6, the following equation holds:

$$\kappa \ln\left(\frac{p'_c}{p'}\right) = \lambda \ln\left(\frac{p'_c}{p'_e}\right) \tag{12}$$

Combining Eq. (11) with (12) yields

$$\ln p'_{cr\_v} = \frac{\Gamma - N}{\lambda} + \frac{\lambda - \kappa}{\lambda} \ln p'_c + \frac{\kappa}{\lambda} \ln p' \tag{13}$$

Substituting Eq. (13) into Eq. (9) yields

$$\frac{q}{Mp'} = 1 + \frac{\beta}{\lambda - \kappa} (\Gamma - N) + \beta \ln\left(\frac{p'_c}{p'}\right) \tag{14}$$

$(\Gamma - N)$ can be determined from the relation of the preconsolidation pressure and the critical state pressure, and is shown as follows:

$$\Gamma - N = (\kappa - \lambda) \ln \frac{2 + R_w}{2} \tag{15}$$

Substituting Eq. (15) into Eq. (14) and noticing $p_{cr}{}' = 2p'/(2 + R_w)$ yields Eq. (3) in the main text.

References

1. Schofield A, Wroth P (1968) Critical state soil mechanics. McGraw Hill, London
2. Roscoe KH, Burland J (1968) On the generalized stress-strain behaviour of wet clay. In: Heyman J, Leckie FA (eds) Engineering plasticity. Cambridge University Press, pp 535–609
3. Dasari G (1996) Modeling of the variation of soil stiffness during sequential construction. Ph.D. Thesis, Cambridge University, UK
4. Mita KA (2002) Constitutive testing of soil on the dry side of critical state. Ph.D. Thesis, National University of Singapore, Singapore
5. Prévost JH (1977) Mathematical modelling of monotonic and cyclic undrained clay behaviour. Int J Numer Anal Meth Geomech 1(2):195–216
6. Mroz Z, Norris V, Zienkiewicz O (1979) Application of an anisotropic hardening model in the analysis of elasto-plastic deformation of soils. Geotechnique 29(1):1–34
7. Al-Tabbaa A (1987) Permeability and stress–strain response of speswhite kaolin. Ph.D. Thesis, University of Cambridge, UK
8. Stallebrass S, Taylor R (1997) The development and evaluation of a constitutive model for the prediction of ground movements in overconsolidated clay. Géotechnique 47(2):235–253
9. Yin Z-Y, Xu Q, Hicher P-Y (2013) A simple critical-state-based double-yield-surface model for clay behavior under complex loading. Acta Geotech 8(5):509–523
10. Whittle AJ (1987) A constitutive model for overconsolidated clays with application to the cyclic loading of friction piles. Ph.D. Dissertation, Massachusetts Institute of Technology, USA
11. Collins IF, Kelly PA (2002) A thermomechanical analysis of a family of soil models. Geotechnique 52(7):507–518
12. Hvorslev M (1960) Physical components of the shear strength of saturated clays. In: Proceedings of ASCE Research Conference on the Shear Strength of Cohesive Soils. Boulder, Colorado, pp 169–273
13. Atkinson JH, Bransby PL (1978) The mechanics of soils: an introduction to critical state soil mechanics. McGraw Hill, London
14. Yao YP, Hou W, Zhou AN (2009) Uh model: three-dimensional unified hardening model for overconsolidated clays. Geotechnique 59(5):451–469
15. Atkinson J (2007) Peak strength of overconsolidated clays. Géotechnique 57(2):127–135
16. Yao YP, Gao ZW, Zhao JD, Wan Z (2012) Modified uh model: constitutive modeling of overconsolidated clays based on a parabolic Hvorslev envelope. J Geotech Geoenviron Eng 138(7):860–868
17. Bryson LS, Salehian A (2011) Performance of constitutive models in predicting behavior of remolded clay. Acta Geotech 6(3):143–154
18. Potts DM, Zdravkovic L (1999) Finite element analysis in geotechnical engineering: theory, vol 1. Thomas Telford, London
19. Atkinson J, Richardson D (1987) The effect of local drainage in shear zones on the undrained strength of overconsolidated clay. Geotechnique 37(3):393–403
20. Pestana JM, Whittle AJ (1999) Formulation of a unified constitutive model for clays and sands. Int J Numer Anal Meth Geomech 23(12):1215–1243
21. Yao YP, Wang ND (2014) Transformed stress method for generalizing soil constitutive models. J Eng Mech 140(3):614–629
22. Zienkiewicz O, Leung K, Pastor M (1985) Simple model for transient soil loading in earthquake analysis. I. Basic model and its application. Int J Numer Anal Meth Geomech 9(5):453–476
23. Banerjee P, Stipho A (1978) Associated and non-associated constitutive relations for undrained behaviour of isotropic soft clays. Int J Numer Anal Meth Geomech 2(1):35–56
24. Banerjee P, Stipho A (1979) An elasto-plastic model for undrained behaviour of heavily overconsolidated clays. Int J Numer Anal Meth Geomech 3(1):97–103
25. Nakai T, Hinokio M (2004) A simple elastoplastic model for normally and over consolidated soils with unified material parameters. Soils Found 44(2):53–70